

# Responses of primary human nasal epithelial cells to COVID-19 vaccine candidate

Phissinee Jakaew,<sup>1</sup> Tuksin Jearanaiwitayakul,<sup>2</sup> Panuwat Midoeng,<sup>3</sup> Promsin Masrinoul,<sup>4</sup> Panya Sunintaboon,<sup>5</sup> Sukathida Ubol<sup>1</sup>

## Abstract

**Background:** Upper respiratory tract is the primary target of SARS-CoV-2. Therefore, nasal immune responses act as the first line of defense against SARS-CoV-2 infection.

**Objective:** We aim to investigate the immune responses of human nasal epithelial cells (HNEpCs) upon stimulation with a COVID-19 vaccine candidate. This candidate named RBD-NPs is composed of SARS-CoV-2 receptor-binding domain (RBD) encapsulated within the *N,N,N*-trimethyl chitosan nanoparticles (TMC-NPs).

**Methods:** HNEpCs were stimulated with RBD-NPs, empty NPs, or soluble RBD at various concentrations. After 24 and 48 h of treatment, cells viability and delivery of the immunogens were assessed using XTT assay and flow cytometry. Levels of cytokines and chemokines in the supernatant were quantified with Bio-plex Human Cytokine Assay. Communication between RBD-NPs-stimulated HNEpCs and monocyte-derived dendritic cells (MoDCs) was assessed through differentiation of MoDCs into mature phenotype.

**Results:** RBD-NPs as high as 100 µg exerted no toxicity to HNEpCs and could effectively be delivered to HNEpCs. Treatment of HNEpCs with RBD-NPs strongly activated production of several pro-inflammatory cytokines, chemokines, Th1-related cytokines and the monocytes/macrophages growth factors. Interestingly, soluble mediators secreted from RBD-NPs treated HNEpCs significantly upregulated the expression of maturation markers (CD80, CD83, CD86 and HLA-DR) on the MoDCs.

**Conclusion:** This study demonstrated that our COVID-19 vaccine candidate drove HNEpCs into immunologically competent cells that not only exerted anti-viral innate immune responses but also potently induced MoDCs maturation.

**Key words:** SARS-CoV-2, COVID-19 vaccine, primary human nasal epithelial cells, RBD, delivery systems

### Citation:

Jakaew, P., Jearanaiwitayakul, T., Midoeng, P., Masrinoul, P., Sunintaboon, P., Ubol, S. (0000). Responses of primary human nasal epithelial cells to COVID-19 vaccine candidate. *Asian Pac J Allergy Immunol*, 00(0), 000-000. <https://doi.org/10.12932/ap-230523-1623>

### Corresponding author:

Sukathida Ubol  
Department of Microbiology, Faculty of Science,  
Mahidol University, Bangkok, 10400, Thailand  
E-mail: sukathida.ubo@mahidol.ac.th

## Introduction

Since 2019, the COVID-19 pandemic caused by the severe acute respiratory syndrome coronavirus (SARS-CoV-2) has affected human lives in many aspects. Unfortunately, its overall impact and termination are yet to be foreseen. SARS-CoV-2 is an airborne coronavirus that initially invades epithelial cells of the mucosal surface in the upper respiratory tract.<sup>1</sup> Specific interaction between SARS-CoV-2 receptor-binding domain (RBD) of the spike glycoprotein and human angiotensin-converting enzyme 2 (ACE2) initiates the first step of SARS-CoV-2 infection.<sup>2</sup>

### Affiliations:

<sup>1</sup>Department of Microbiology, Faculty of Science, Mahidol University, Bangkok, Thailand

<sup>2</sup>Department of Clinical Pathology, Faculty of Medicine Vajira Hospital, Navamindradhiraj University, Bangkok, Thailand

<sup>3</sup>Division of Pathology, Army Institute of Pathology, Phramongkutklao Hospital, Bangkok, Thailand

<sup>4</sup>Center for Vaccine Development, Institute of Molecular Biosciences, Mahidol University, Nakhon Pathom, Thailand

<sup>5</sup>Department of Chemistry, Faculty of Science, Mahidol University, Salaya, Nakhon Pathom, Thailand

Thus, RBD is one of the key targets for COVID-19 vaccine development owing to its major role in mediating viral entry. RBD also contains multiple conformational neutralizing epitopes that induce neutralizing antibodies and activate specific cellular immune responses.<sup>3</sup>

At present, approved COVID-19 vaccines for emergency uses have been designed for traditional intramuscular injection. This excellently stimulates systemic immune response but fails or poorly induces local mucosal immune system. Since respiratory tract serves as the primary target of SARS-CoV-2, protective responses against the virus in this organ should be crucial to prevent its infection and transmission. Nasal cavity is well suited for vaccine administration because immunogens will be recognized by several types of TLRs on the epithelial cells, resulting in production of anti-viral mediators including pro-inflammatory cytokines and chemokines. These mediators from nasal epithelium will then stimulate mucosal immune responses through nasopharynx-associated lymphoid tissue (NALT), which contains networks of immune cells including dendritic, T and B cells.<sup>4-5</sup> In addition, intranasal administration is a non-invasive, needle-free route which is suitable for mass vaccination.<sup>6</sup> Thus, intranasal vaccination may serve as an alternative strategy to control SARS-CoV-2 epidemic.

Madharan M, et. al. had recently investigated phase I trial of intranasal ChAdOxI vaccine against COVID-19 and had revealed some disappointing results. They reported that naïve individuals who received two intranasal doses of ChAdOxI failed to develop mucosal IgA or Ig responses. While those who received the intranasal ChAdOxI vaccine as a booster did not elicit strong mucosal antibody response.<sup>7</sup> These might be resulted from an inappropriate vector used in the vaccine platform. As an attenuated-chimeric virus which utilizes simian adenovirus as a vector, the intranasal ChAdOxI vaccine may not effectively penetrate the human respiratory mucosa due to the low expression of host receptors for the simian.<sup>8</sup> In contrast, a nasal spray vaccine, Bharat Biotech's iNCOVACC, had recently been approved by the India's Central Drugs Standard Control Organization due to its potent immunogenicity.<sup>9</sup> In addition, a booster of the orally inhaled version of the adenovirus type5 vector encoding SARS-CoV-2 spike protein had been demonstrated to induce stronger neutralizing antibody responses when compared to the intramuscular dose.<sup>10</sup> In addition, although positive outcomes of intranasal vaccination in animal models had been observed, its failure to induce mucosal immune responses in human highlights the need for alternative preclinical models for the vaccine testing.

In this study, the primary human nasal epithelial cells (HNEpCs) have been chosen as an *in vitro* model to investigate immune responses and cytotoxicity induced by a COVID-19 candidate vaccine. Our vaccine candidate named RBD-NPs contains RBD encapsulated in adjuvanted-nanodelivery system; *N,N,N*-trimethyl chitosan nanoparticles (TMC-NPs). We recently reported that TMC-NPs are a promising adjuvant and delivery system for mucosal subunit vaccine.<sup>11-14</sup> This is due to its mucoadhesive property, the controlled release of immunogens at cellular level, and the capability to enhance both local innate and systemic immunity.<sup>11-12</sup> Innate immune responses of HNEpCs upon RBD-NPs stimulation were investigated. The ability of RBD-NPs-treated HNEpCs to drive the immature MoDCs into mature phenotype was monitored.

## Methods

### *Cultivation of primary human nasal epithelial cells (HNEpCs)*

HNEpCs (C-12620, PromoCell, Germany) were cultured in the commercial airway cell growth medium (PromoCell) at 37°C with 5% CO<sub>2</sub>, using culture flasks coated with human collagen solution (50 µg/mL, Advanced BioMatrix, USA).

### *Preparation of SARS-CoV-2 RBD protein*

Recombinant RBD protein was purified using the affinity chromatography on Nickel-chelate resin (Invitrogen). Purified RBD was confirmed with immunoblotting using rabbit anti-SARS-CoV-2 RBD polyclonal antibody (Sino Biological, China). The level of contaminated endotoxin in the purified RBD protein was quantified using the Limulus amoebocyte lysate assay (QCL-1000; Pierce, Rockford, IL, USA) and found to be < 0.1 EU/mg.

### *Formulation and characterization of RBD-NPs*

RBD-NPs were constructed using ionotropic gelation method as previously described.<sup>13</sup> Briefly, sodium tripolyphosphate (TPP) solution containing RBD protein (0.3 mg/mL) was mixed with an aqueous solution of TMC (1 mg/mL) containing 1% Tween 80 in HEPES buffer. After centrifugation at 10,000 × g for 10 min, supernatant with unbound proteins was collected for loading efficiency calculation.<sup>13</sup> Entrapped RBD in RBD-NPs was subjected to immunoblotting using anti-RBD antibody. Physical properties of RBD-NPs (size, polydispersity and zeta potential) were assessed using Zetasizer (Malvern Instrument, UK).

### *Cytotoxicity assay*

HNEpCs monolayer cultures were washed with PBS before being treated with various concentrations of empty NPs or RBD-NPs (25 to 200 µg/mL), 10% DMSO or medium. The viability of the treated HNEpCs was quantitated using XTT assay (Sigma Aldrich, USA) at 24 and 48 h after treatment.

### Cellular uptake of RBD- NPs

To examine the cellular uptake of RBD-NPs, HNEpCs monolayer cultures were treated with medium, soluble RBD (7 and 28  $\mu\text{g}/\text{mL}$ ) or RBD-NPs (25 and 100  $\mu\text{g}/\text{mL}$  which contained 7 and 28  $\mu\text{g}/\text{mL}$  of entrapped RBD, respectively). At 24 and 48 h of treatment, cells were washed, fixed and permeabilized with Cytofix/Cytoperm™ solution kit (BD biosciences). Intracellular RBD antigen was stained with rabbit anti-SARS-CoV-2 RBD polyclonal antibody (Sino Biological, China) followed by Alexa Fluor 488-conjugated goat anti-rabbit antibody (Invitrogen). The percentage of fluorescence positive cells and mean fluorescence intensity (MFI) were quantitated using flow cytometry.

### Cytokine and chemokine production

HNEpCs were washed with PBS before being treated with RBD-NPs (25 and 100  $\mu\text{g}/\text{mL}$ ), empty NPs (25 and 100  $\mu\text{g}/\text{mL}$ ), soluble RBD (28  $\mu\text{g}/\text{mL}$ ) or medium. Supernatants were harvested at 24 and 48 h to quantify the levels of seventeen cytokines and chemokines (IL-6, IL-1 $\beta$ , TNF- $\alpha$ , IL-2, IL-12, IL-17, IFN- $\gamma$ , IL-4, IL-5, IL-10, IL-13, MCP-1, MIP-1 $\beta$ , IL-8, G-CSF, GM-CSF and IL-7) using Bio-plex human cytokine assay kit (Bio-Rad, Hercules, CA, USA). The amount of type I interferon (IFN- $\alpha$ ) was quantified separately using an ELISA kit (VerKine™, USA).

### Isolation and cultivation of MoDCs

Human peripheral blood mononuclear cells (PBMCs) were isolated from buffy coat using Lymphoprep (Axis-Shield, Oslo, Norway). The use of PBMCs from healthy donors has been approved by the Ethic Committee on Human Rights Related to Human experimentation, Mahidol University, Bangkok, Thailand (protocol: 2022/279.1710), in accordance to ethical standards of the Declaration of Helsinki. CD14<sup>+</sup> monocytes were subsequently purified using magnetic cell isolation (Miltenyi Biotech, USA). The purified monocytes were differentiated in MoDCs in RPMI-1640 medium following the previously described method.<sup>14</sup> Flow cytometry (CytoFLEX, Beckman Coulter, IN, USA) was used to confirm the differentiation of MoDCs using CD209-specific antibody (R&D Systems, USA).

### The effects of HNEpCs-derived immune mediators on MoDCs maturation

HNEpCs were treated with RBD-NPs (25 and 100  $\mu\text{g}/\text{mL}$ ), empty NPs (25 and 100  $\mu\text{g}/\text{mL}$ ), soluble RBD (28  $\mu\text{g}/\text{mL}$ ) or medium. Supernatant of treated-HNEpCs harvested at 48 h was then added onto the MoDCs cultures. After 24 and 28 h, treated MoDCs were stained with specific antibodies to detect the maturation markers (CD80, CD83, CD86 and HLA-DR) using flow cytometry (CytoFLEX, Beckman Coulter, IN, USA).

### Statistical analysis

All data shown were statistically analyzed from at least three independent experiments. Results were reported as mean  $\pm$  SD. Statistical analysis was performed using student's *t*-test. Statistically differences were considered when the *p*-value is less than 0.05.

## Results

### Characterization of RBD- NPs

SARS-CoV-2 RBD proteins were encapsulated into TMC NPs via ionotropic gelation to generate RBD-NPs. The physical properties of the RBD-NPs were then determined. The RBD-NPs showed an average diameter of  $386.5 \pm 58.96$  nm, with a narrow size distribution of  $0.407 \pm 0.019$  and positively-charged surface of  $+12.9 \pm 0.65$  mV (Table 1).

**Table 1. The physical properties of RBD-NPs and empty NPs, including particle size, polydispersity (PDI) and zeta-potential, were determined using Zetasizer.**

Nanoparticles	Particle size (nm)	Polydispersity (PDI)	Zeta-potential (mV)
empty NPs	$362.7 \pm 44.19$	$0.374 \pm 0.021$	$+15.4 \pm 0.306$
RBD-NPs	$386.5 \pm 58.96$	$0.407 \pm 0.019$	$+12.9 \pm 0.651$

We found that RBD proteins were encapsulated within TMC NPs with remarkably high loading efficiency of  $93.57 \pm 8.64\%$ . RBD-NPs at 25 and 100  $\mu\text{g}/\text{mL}$  were found to contain 7 and 28  $\mu\text{g}/\text{mL}$  of RBD, respectively. Moreover, RBD released from NPs was found to strongly interacted with anti-RBD antibody used in immunoblotting (Figure 1). These results indicated that ionotropic gelation method could be effectively used to encapsulate RBD proteins within TMC NPs without disrupting the antigenicity detected by an anti-SARS-CoV-2 antibody (Cat# 40592-V05H).

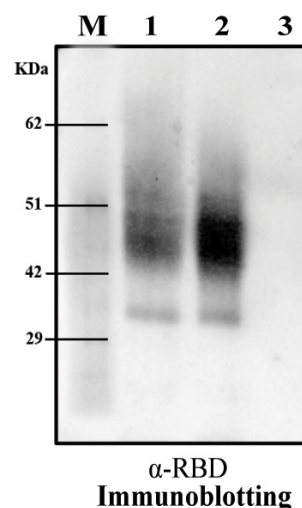


**Figure 1. Entrapped RBD protein in TMC NPs detected by immunoblotting using an anti-RBD antibody. Lane1; RBD-NPs, Lane 2; soluble RBD, Lane3; empty NPs.**

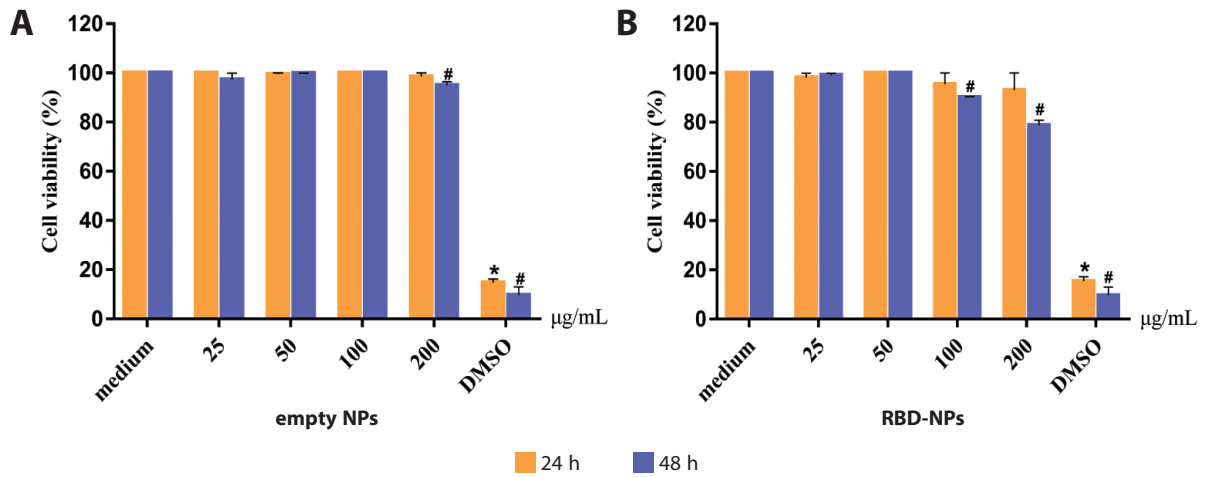


**Figure 2. Toxicity of RBD-NPs on HNEpCs.** HNEpCs were treated with (A) empty NPs or (B) RBD-NPs at various concentrations (25 to 200 µg/mL) or 10% DMSO (positive control) or medium (negative control) for 24 and 48 h. Cell viability was quantitated using XTT assay. All data are presented as mean ± SD. \* and # indicate significant differences ( $p < 0.05$ ) between empty NPs or RBD-NPs treatments compared to that of the medium control at 24 h and 48 h, respectively.

**Cytotoxicity assay**

To determine the safety of RBD-NPs at cellular level, the toxicity of RBD-NPs or empty NPs on HNEpCs was assessed. The cytotoxicity was not detected at 24 h of treatment. At 48 h after treatment, however, cell viabilities were determined to be 100% and  $90.12 \pm 0.52\%$  following empty NPs and RBD-NPs treatment at 100 µg/mL, respectively (Figure 2). Treatments with RBD-NPs concentrations lower than 100 µg/mL exerted undetectable toxicity. Hence, RBD-NPs and empty NPs at 100 µg/mL were chosen for the further experiments.

**Cellular uptake of RBD-NPs**

The efficiency of nanoparticles in delivering RBD into HNEpCs was investigated. As shown in Figure 3, HNEpCs treated with 100 µg/mL of RBD-NPs showed a significant ( $p < 0.05$ ) higher percentage of RBD<sup>+</sup> HNEpCs after treatment and stronger mean fluorescence intensity (MFI) compared to that of the soluble RBD treatment (28 µg/mL). Treatment with RBD-NPs at 100 µg/mL showed  $64.03 \pm 1.69\%$  and  $64.85 \pm 0.30\%$  RBD<sup>+</sup> cells at 24 and 48 h after treatment, respectively. Moreover, treatment with this condition revealed mean fluorescence intensities at  $186,427.2 \pm 11,811.51$  and  $190,113.5 \pm 23,028.84$  for 24 and 48 h after treatment, respectively (Figure 3A-B). Meanwhile, soluble RBD

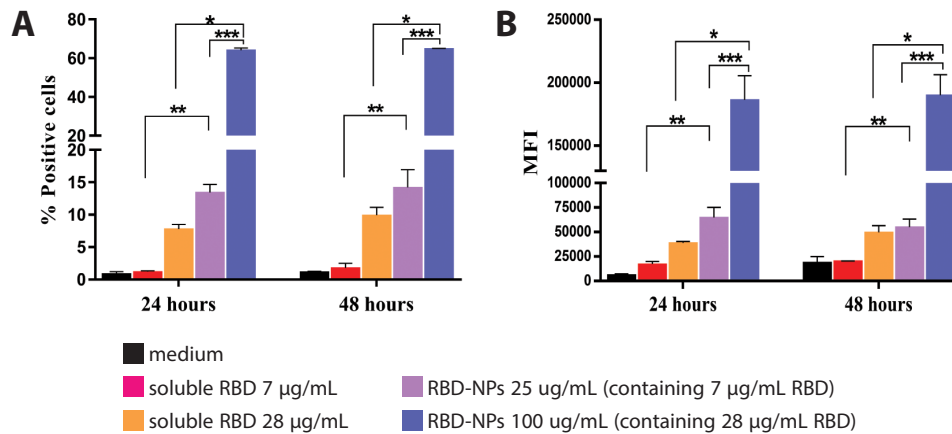


**Figure 3. Delivery of RBD into HNEpCs.** HNEpCs were treated with various concentrations of RBD-NPs, soluble RBD or medium. At 24 and 48 h of treatment, the harvested cells were intracellularly stained with anti-RBD antibody before being analyzed using flow cytometry. (A) Percentage of RBD<sup>+</sup> cells. (B) Mean fluorescence intensity (MFI). (C) Dot plot analysis of HNEpCs treated with isotype control, soluble RBD at 28 µg/mL and RBD-NPs at 100 µg/mL at 48 h after treatment. \*indicates significant differences between 100 µg/mL of RBD-NPs and 28 µg/mL of soluble RBD. \*\*indicates significant differences between 25 µg/mL of RBD-NPs and 7 µg/mL of soluble RBD. \*\*\*indicates significance difference between RBD-NPs at 25 and 100 µg/mL ( $p < 0.05$ ).

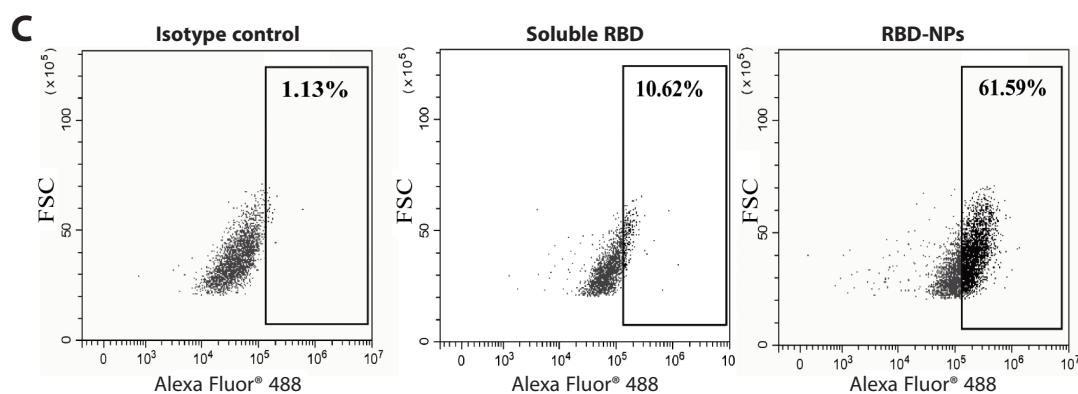


**Figure 3. (Continued)**

treatment (28 µg/mL) resulted in only  $7.80 \pm 0.96\%$  and  $9.94 \pm 1.71\%$  RBD<sup>+</sup> cells at 24 and 48 h of treatment, respectively. The soluble protein treatment could slightly deliver immunogens into HNEpCs, but not significantly higher than that of the control treatment. These results indicated that TMC NPs could efficiently facilitate the delivery of RBD antigens into HNEpCs.

#### **Cytokines and chemokines production in response to RBD-NPs**

To investigate the immunostimulatory effect of RBD-NPs, HNEpCs cultures were treated with RBD-NPs (25 or 100 µg/mL), empty NPs (25 or 100 µg/mL), or soluble RBD (28 µg/mL). Supernatants were harvested at 24 and 48 h of treatment and subjected to cytokine and chemokine quantification. Here, we revealed that the productions of cytokines, chemokines and growth factors were upregulated in the supernatants of HNEpCs treated with RBD-NPs (100 µg/mL) at 24 and 48 h of treatment (**Figure 4**). These included pro-inflammatory cytokines (IL-6, TNF-α and IL-1β), chemokines (IL-8 and MIP-1β), Th-1 related cytokines (IFN-γ and IL-12) and growth factors (G-CSF and GM-CSF). Upon treatment, the production of IL-6 was significantly stimulated at 48 h after treatment. This stimulation occurred in a dose- and time-dependent manner. TNF-α was significantly induced in HNEpCs treated with RBD-NPs (100 µg/mL) at 24 h after treatment and was gradually downregulated at 48 h of treatment. Although not very high, the level of IL-1β in the supernatant was significantly upregulated in response to RBD-NPs (100 µg/mL).

For chemokines, IL-8 and MIP-1β were produced in dose- and time- dependent manner in HNEpCs treated with RBD-NPs (100 µg/mL) comparing to those of the other groups. As shown in **Figure 4B**, productions of IL-8 and MIP-1β peaked at 48 h after treatment, at which our study terminated. The means of production were  $5,288.6 \pm 3472.08$  and  $18.13 \pm 9.41$  pg/mL for IL-8 and MIP-1β, respectively. In terms of growth factor, G-CSF production was induced in all treated conditions at 24 h and peaked at 48 h after treatment. As expected, RBD-NPs were the most potent inducers of G-CSF among tested stimuli. Interestingly, soluble RBD and RBD-NPs strongly stimulated the production of GM-CSF when compared to those of the other stimuli tested. This could be evidenced by the levels

of GM-CSF in the supernatant at 24 and 48 h of treatment. Results shown in **Figure 4C** suggested that RBD was a strong inducer of growth factors.

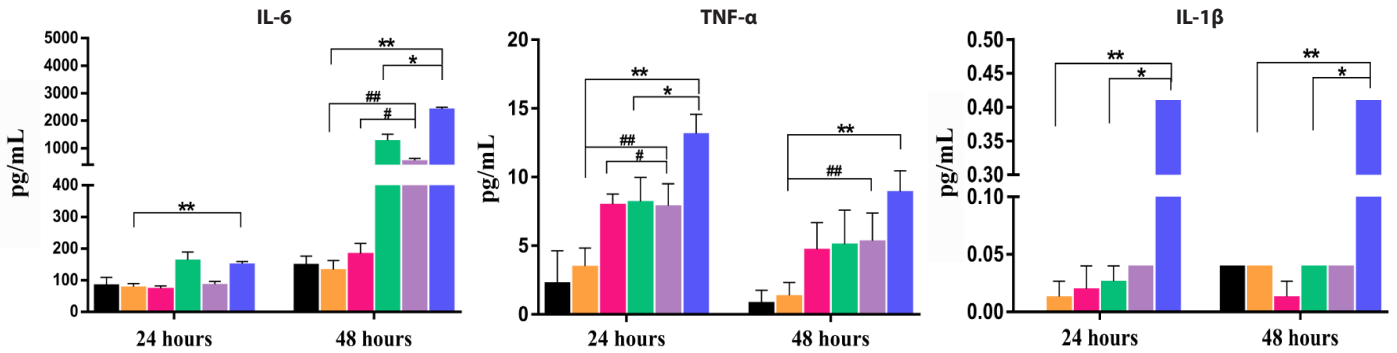
For Th-1 related cytokines, the production of IFN-γ and IL-12 were also determined. As expected, treatment with RBD-NPs (100 µg/mL) stimulated the highest level of IL-12 production, but not IFN-γ production, at 24 h of treatment (**Figure 4D**).

#### **The effects of HNEpCs-derived immune mediators on MoDCs maturation**

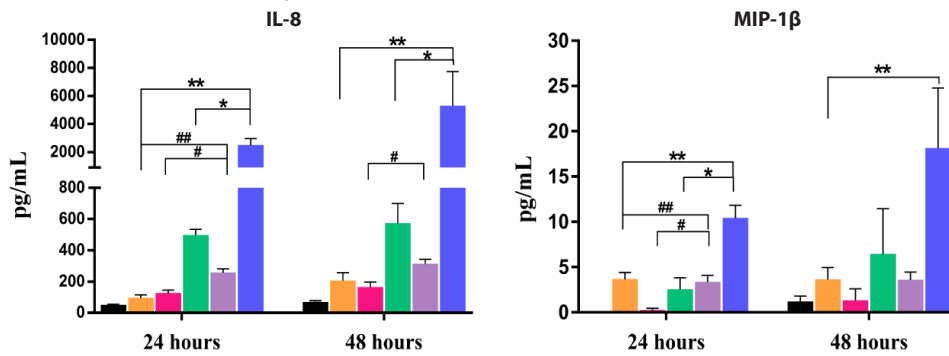
We next investigated the possible roles of soluble mediators secreted from RBD-NPs- treated HNEpCs in adaptive immune response. Since dendritic cells provide the important cross-talking between the innate and adaptive immune responses, the impact of the secreted mediators on the dendritic cell maturation was assessed. Supernatants obtained from HNEpCs stimulated with RBD-NPs, empty NPs, soluble RBD protein, or medium were subjected to MoDCs treatment. The expressions of MoDCs maturation markers were monitored using flow cytometry.

As shown in **Figure 5**, the expressions of CD80, CD83, CD86 and HLA-DR were upregulated in response to treatment with soluble mediators secreted from RBD-NPs-treated HNEpCs. For CD80 expression, treatment with the supernatant from RBD-NPs-treated culture was able to upregulate CD80 expression on the surface of MoDCs within 24 h and peaked by 48 h of the treatment. Stimulation of CD80 expression was revealed in both the percentages of positive cells and the intensity of expression per cell (MFI) in which > 80% of MoDCs upregulated CD80 expression (MFI =  $20,353.9 \pm 3,877.45$  and  $27,214.07 \pm 2,226.33$  for 25 and 100 µg/mL RBD-NPs groups at 48 h of treatment, respectively) upon stimulation by supernatant from RBD-NPs treated cells. Similarly, expression of CD86 was induced by mediators secreted from RBD-NPs-treated HNEpCs. This was revealed through the data that  $42.56 \pm 3.27\%$  and  $58.91 \pm 14.52\%$  of treated MoDCs upregulated CD86 expression with MFI were  $30,523.8 \pm 1,035.20$  and  $41,922.35 \pm 8,179.17$  for 25 and 100 µg/mL RBD-NPs groups at 48 h of experimentation, respectively. Whereas surface expression of CD83 by MoDCs treated with mediators from RBD-NPs treated medium was significantly higher ( $p < 0.05$ ) than that of mediators

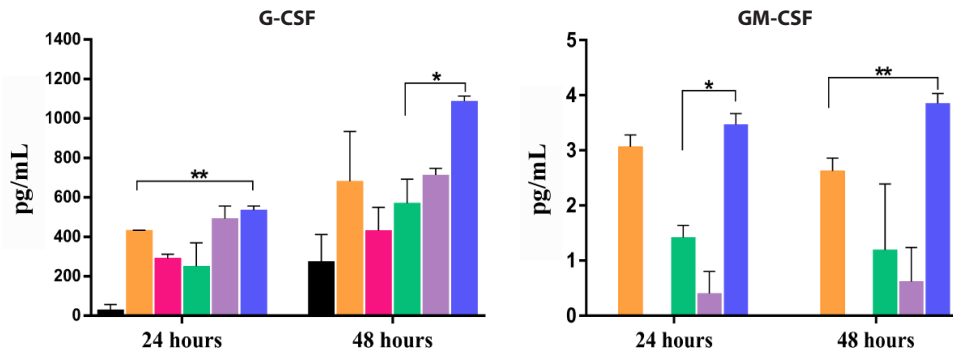
**A Pro-inflammatory cytokines (IL-6, TNF- $\alpha$  and IL-1 $\beta$ )**



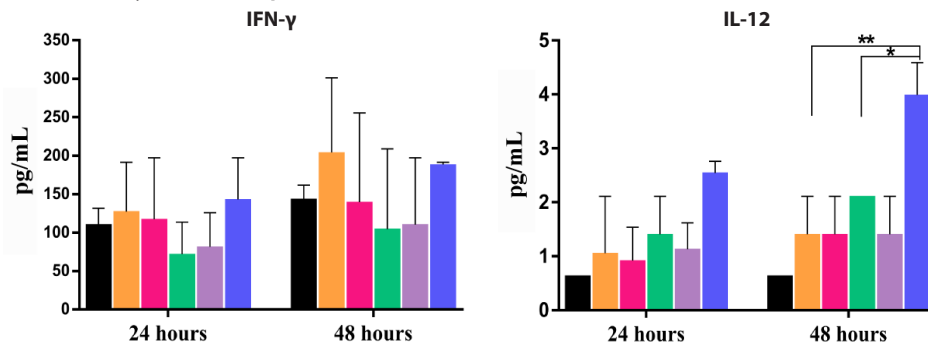
**B Chemokines (IL-8 and MIP-1 $\beta$ )**



**C Growth Factors (G-CSF and GM-CSF)**



**D Th-1 related cytokines (IFN- $\gamma$  and IL-12)**



medium     
  empty NPs 25  $\mu$ g/mL     
  RBD-NPs 25  $\mu$ g/mL (containing 7  $\mu$ g/mL RBD)

soluble RBD 28  $\mu$ g/mL     
  empty NPs 100  $\mu$ g/mL     
  RBD-NPs 100  $\mu$ g/mL (containing 28  $\mu$ g/mL RBD)

**Figure 4. Production of cytokines and chemokines in response to RBD-NPs.** HNEpCs were treated with RBD-NPs (25  $\mu$ g/mL and 100  $\mu$ g/mL), empty NPs (25  $\mu$ g/mL and 100  $\mu$ g/mL), soluble RBD (28  $\mu$ g/mL) or medium. The level of (A) pro-inflammatory cytokines, (B) chemokines, (C) growth factors and (D) Th-1 related cytokines were quantified using Bio-plex human cytokine assay kit. All data were represented as mean  $\pm$  SD. # and \* indicate significant difference between HNEpCs treated with RBD-NPs and empty NPs at 25 or 100  $\mu$ g/mL, respectively ( $p < 0.05$ ). ## and \*\* indicate significant difference between HNEpCs treated with soluble RBD (28  $\mu$ g/mL) and HNEpCs treated with RBD-NPs at 25 or 100  $\mu$ g/mL, respectively ( $p < 0.05$ ).

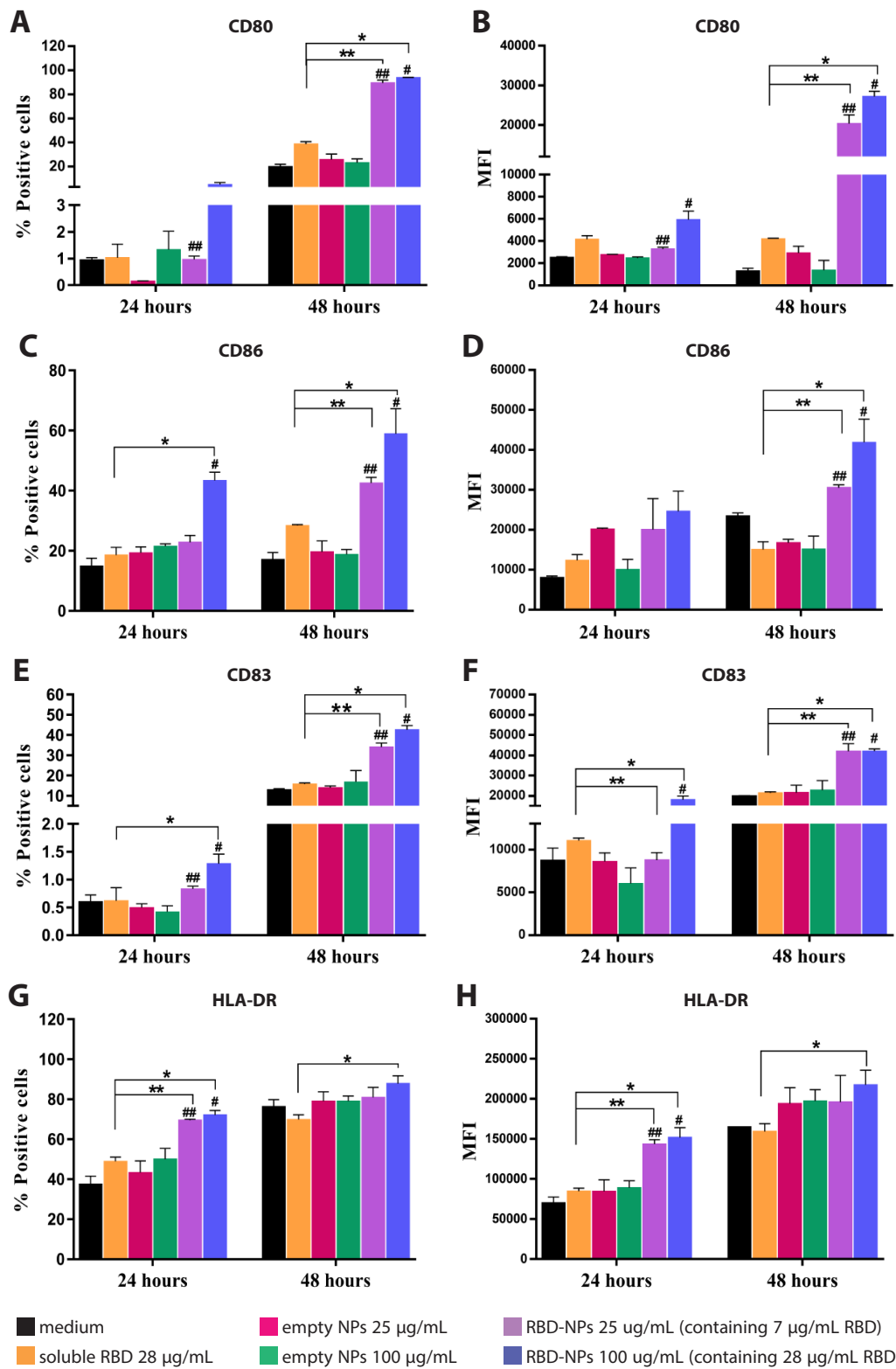


**Figure 5. Expression of maturation markers on MoDCs upon treatment with soluble mediators secreted by RBD-NPs-treated HNEpCs at 24 and 48 h after treatment.** HNEpCs were treated with RBD-NPs (25 µg/mL and 100 µg/mL), empty NPs (25 µg/mL and 100 µg/mL), soluble RBD (28 µg/mL) or medium. Supernatants from HNEpCs were harvested at 48 h and were used to treat MoDCs. MoDCs maturation markers including CD80 (A and B), CD86(C and D), CD83 (E and F) and HLA-DR (G and H) were monitored at 24 h and 48 h of treatment using flow cytometry. The expression of MoDCs maturation markers was presented as mean fluorescence intensity (MFI) and percentages of positive cells. Histogram represents the mean of 3 independent experiments (n = 3). \* and \*\* indicate significant differences between soluble mediators secreted by the cells treated with soluble RBD (28 µg/mL) and RBD-NPs at 100 or 25 µg/mL, respectively. # indicates significant differences between soluble mediators secreted by the cells treated with RBD-NPs and empty NPs at 100 µg/mL. ## indicates significant differences between soluble mediators secreted by the cells treated with RBD-NPs and empty NPs at 25 µg/mL ( $p < 0.05$ ).

from other treated conditions at 24 and 48 h of treatment (Figure 5E-F). Expression of HLA-DR was upregulated in MoDCs upon treatment with mediators from RBD-NPs-treated HNEpCs (Figure 5, G-H). These results suggested that soluble mediators secreted from HNEpCs treated with RBD-TMC NPs were able to drive the immature MoDCs into the mature phenotype.

## Discussion

SARS-CoV-2 is a mucosal pathogen that spreads through droplets, resulting in a high rate of transmission in human population. Upper respiratory tract, including nasal cavity, is the major entry site for SARS-CoV-2.<sup>15</sup> Therefore, the nasal route is considered as an attractive route for vaccine administration to promote mucosal anti-SARS-CoV-2 response. Epithelial cells of the nasal mucosa can sense immunogens and initiate innate immune responses through the production of several cytokines and chemokines. These cells also provide signals to antigen-presenting cells (APCs) in NALTs, resulting in stimulation of adaptive immune response.<sup>4</sup> Another word is intranasal vaccination will not only enable non-invasive immunization, but also promote both systemic and local mucosal responses. This can control viral infection on the transmission route.<sup>16</sup> However, most currently approved COVID-19 vaccines are administered via the intramuscular route, which induce a robust systemic immune response but are inefficient in inducing local mucosal immunity. This results in incomplete protection against infection and transmission.

In this study, we investigated the responses of human nasal epithelial cells toward stimulation of a COVID-19 vaccine candidate, RBD-NPs. SARS-CoV-2 RBD protein was chosen as the target antigen since it contains abundant conformational epitopes to promote both humoral and cellular immune responses.<sup>17</sup> In this study, RBD protein was successfully encapsulated into TMC NPs with high loading efficiency (> 93%). Immunoblotting indicated that the antigenicity of RBD was unaltered after the encapsulation.

Small size and positively-charged surface of the nanoparticles are crucial for the immunogen delivery efficiency. Small-sized particles can effectively penetrate into the epithelial cells. It has been reported that the particle with sizes smaller than 1  $\mu\text{m}$  are suitable for up-taking by mucosal M cells.<sup>18</sup> The positively-charged surface not only efficiently interacts with the negatively-charged epithelial surface, but also facilitates transepithelial transportation of encapsulated antigens by widening tight junctions between epithelial cells.<sup>19-20</sup> Our RBD-NPs were small-sized ( $386.5 \pm 58.96$  nm) with positively-charged surface ( $12.9 \pm 0.651$  mV). With these properties, the particles aid efficient internalization of RBD. This evidenced by higher percentages of RBD positive cells and higher amount of RBD internalized in each cell in the RBD-NPs treated group comparing to the soluble RBD treatment. Notably, the percentage of positive cells and MFI at

24 and 48 h of RBD-NPs treatment were not different. This suggested that penetration of RBD-NPs into HNEpCs reached the maximum levels within 24 h of treatment. The mechanism of cellular uptake was not investigated in the present study. However, we believe that the uptake of RBD-NPs may be mediated through the interaction between the positively charged surface of NPs and the negatively charged cell membrane. The low cytotoxicity was demonstrated in the cells treated with RBD-NPs and empty NPs, suggesting that TMC-NPs should serve as a safety vaccine delivery system for human nasal epithelium and possibly for intranasal vaccination.

Both innate and adaptive immune responses of the respiratory tract have been shown to regulate the outcome of SARS-CoV-2 infection.<sup>21</sup> In our present study, treatment of HNEpCs with RBD-NPs could elicit both innate and adaptive immune responses, as indicated by the increased production of pro-inflammatory cytokines (IL-6, TNF- $\alpha$  and IL-1 $\beta$ ), chemokines (IL-8 and MIP-1 $\beta$ ), Th-1 related cytokines (IFN- $\gamma$  and IL-12) and growth factors (G-CSF and GM-CSF).

Activation of pro-inflammatory cytokines during the early phase of virus infection is crucial for activation of innate and adaptive immune responses. The upregulation of IL-1 $\beta$  upon RBD-NPs stimulation indicated inflammatory activation. Once IL-1 $\beta$  binds to IL-1R, it induces transcriptional program, resulting in increased production of several inflammatory mediators including IL-6 and TNF- $\alpha$ .<sup>22</sup> During early viral infection, activated inflammasome initiates proper innate immune response against the viral infection. In addition, inflammasome mediators also induce the expression of co-stimulatory molecules on the antigen presenting cells. These molecules are essential for subsequent adaptive immune response activation. Elevated IL-6 promotes the survival of phagocytic neutrophils and the differentiation of monocytes into macrophages. IL-6 also promotes T cell proliferation and regulates antigen-dependent B cell differentiation.<sup>23</sup> Upregulated TNF- $\alpha$  involves in inflammatory responses, and also increases IL-6 production. TNF- $\alpha$  induces a cascade of inflammatory responses by binding to Type 1 receptors (TNF1) and Type 2 receptors (TNF2). Activation of TNFR1 results in the formation of Complexes I and II, while that of TNFR2 results in Complex I generation. This functional complex I will subsequently triggers a signaling cascade that activates NF- $\kappa\text{Bs}$  and MAPKs, resulting in inflammation, tissue damage, host defense, cell survival and cell proliferation. The functional complex II (IIa and IIb) induces apoptosis through caspase-8, while complex IIc can activate MLKL which leads to inflammation and necroptosis.<sup>24</sup>

For chemokine production, elevated IL-8 and MIP-1 $\beta$  were also detected in RBD-NPs treated cells. IL-8 is associated with recruitment, activation and accumulation of neutrophils as part of the inflammation response,<sup>25</sup> whereas MIP-1 $\beta$  promotes the recruitment of various innate and adaptive immune cells.<sup>26</sup>

In terms of growth factors, we also found G-CSF and GM-CSF productions upon treatment with RBD-NPs. G-CSF can induce MoDC differentiation and granulocyte proliferation and can also activate the effector functions of mature neutrophils.<sup>27</sup> GM-CSF facilitates communication between tissue-invading lymphocytes and myeloid cells by stimulating the production of pro-inflammatory cytokines and chemokines such as IL-6 and TNF. It also plays an important role in inducing Th17 response, which is significant for host defense against extracellular pathogens such as bacteria, fungi and virus at the mucosal surface.<sup>28-29</sup>

For Th-1 related cytokine production, increased production of IL-12 was observed in HNEpCs stimulated with RBD-NPs. IL-12 has been shown to inhibit viral replication by inducing IFN- $\gamma$  activity, as well as improving CD8<sup>+</sup> T cell response.<sup>28</sup> Taken together, we observed increased levels of cytokines and chemokines in HNEpCs in response to RBD-NPs, suggesting that RBD-NPs are able to trigger both cellular and soluble forms of anti-viral innate responses.

Apart from the innate immune response, airway epithelium also induces adaptive immune response by interacting with antigen presenting cells underneath the mucosal layer.<sup>30</sup> Here we demonstrated that soluble mediators from RBD-NPs-treated HNEpCs were able to drive the maturation of MoDCs, which was demonstrated by the upregulation of CD80, CD83, CD86 and HLA-DR expression. This may be due to the fact that RBD-NPs-treated HNEpCs secreted IL-6, TNF- $\alpha$ , IL-1 $\beta$ , IL-8, MIP-1 $\beta$ , IFN- $\gamma$ , IL-12, G-CSF and GM-CSF. These cytokines and chemokines are not only involved in the inflammatory response but also participate in DCs activation. For example, a combination of TNF- $\alpha$ , IL-6, IL-1 $\beta$  and PGE2 has been reported to activate DCs maturation via activation of inflammatory response genes. A combination of IL-1 $\beta$ , TNF- $\alpha$ , IFN- $\alpha$ , and IFN- $\gamma$  can activate DCs maturation through the activation of indoleamine-2,3-deoxygenase (IDO), while IFN- $\gamma$  itself can promote DCs maturation via JAKs, TYK2 and STAT1/2 pathways.<sup>31-33</sup> The combinations of these various mediators provide the environment that is suitable for DCs to undergo differentiation and maturation.

In conclusion, as a COVID-19 vaccine candidate, RBD-NPs not only act as an effective delivery system but also exert low toxicity to epithelium lining nasal cavity. Importantly, this platform strongly activates production of an anti-viral innate mediators such as IL-6, TNF- $\alpha$ , IL-1 $\beta$ , IL-8, MIP-1 $\beta$ , IFN- $\gamma$ , IL-12, G-CSF and GM-CSF which consequently drive immature dendritic cells to mature into the functional phenotype. Altogether, our results demonstrated the high potential of RBD-NPs in activating protective mucosal responses against SARS-CoV-2 in human.

## Conflicts of Interest

The authors affirm that there is no conflict of interest associated with the publication of this article.

## Acknowledgements

This work was supported by the National Vaccine Institute, Thailand to Ubol S (grant number 2563.1/9).

## References

- Ryu G, Shin HW. Sars-cov-2 infection of airway epithelial cells. *Immune Netw.* 2021;21(1):1-16.
- Bestle D, Heindl MR, Limburg H, van Lam van T, Pilgram O, Moulton H, et al. TMPRSS2 and furin are both essential for proteolytic activation of SARS-CoV-2 in human airway cells. *Life Sci Alliance.* 2020;3(9):1-14.
- Fast E, Chen B. Potential T-cell and B-cell Epitopes of 2019-nCoV. 2020;1-13.
- Gallo O, Locatello LG, Mazzoni A, Novelli L, Annunziato F. The central role of the nasal microenvironment in the transmission, modulation, and clinical progression of SARS-CoV-2 infection. *Mucosal Immunol.* 2021;14(2):305-16.
- Sha Q, Truong-Tran AQ, Plitt JR, Beck LA, Schleimer RP. Activation of airway epithelial cells by toll-like receptor agonists. *Am J Respir Cell Mol Biol.* 2004;31(3):358-64.
- Mangla B, Javed S, Sultan MH, Ahsan W, Aggarwal G, Kohli K. Nanocarriers-Assisted Needle-Free Vaccine Delivery Through Oral and Intranasal Transmucosal Routes: A Novel Therapeutic Conduit. *Front Pharmacol.* 2022; 12:1-20.
- Madhavan M, Ritchie AJ, Aboagye J, Jenkin D, Provstgaard-Morys S, Tarbet I, et al. Tolerability and immunogenicity of an intranasally-administered adenovirus-vectored COVID-19 vaccine: An open-label partially-randomised ascending dose phase I trial. *eBioMedicine.* 2022; 85:104298.
- Weaver EA, Camacho ZT, Hillestad ML, Crosby CM, Turner MA, Guenzel AJ, et al. Mucosal vaccination by adenoviruses displaying reovirus sigma 1. *Virology.* 2015; 482:60-6.
- Singh C, Verma S, Reddy P, Diamond MS, Curiel DT, Patel C, et al. Phase III Pivotal comparative clinical trial of intranasal (iNCOVACC) and intramuscular COVID 19 vaccine (Covaxin®). *npj Vaccines.* 2023; 8(1).
- Langel SN, Johnson S, Martinez CI, Tedjakusuma SN, Peinovich N, Dora EG, et al. Adenovirus type 5 SARS-CoV-2 vaccines delivered orally or intranasally reduced disease severity and transmission in a hamster model. *Sci Transl Med.* 2022;14(658).
- Nantachit N, Sunintaboon P, Ubol S. Responses of primary human nasal epithelial cells to EDIII-DENV stimulation: The first step to intranasal dengue vaccination. *Virology.* 2016;13(1):1-8.
- Jearanaiwitayakul T, Limthongkul J, Kaofai C, Apichirapokey S, Chawengkirttikul R, Sapsutthipas S, et al. The STING Ligand and Delivery System Synergistically Enhance the Immunogenicity of an Intranasal Spike SARS-CoV-2 Vaccine Candidate. *Biomedicines.* 2022; 10(5).
- Jearanaiwitayakul T, Sunintaboon P, Chawengkirttikul R, Limthongkul J, Midoeng P, warit S, et al. Nanodelivery system enhances the immunogenicity of dengue-2 nonstructural protein 1, DENV-2 NS1. *Vaccine.* 2020;38(43):6814-25.
- Rungrojcharoenkit K, Sunintaboon P, Ellison D, Macareo L, Midoeng P, Chaisuwirat P, et al. Development of an adjuvanted nanoparticle vaccine against influenza virus, an in vitro study. *PLoS One.* 2020;15:1-18.
- Ahn JH, Kim JM, Hong SP, Choi SY, Yang MJ, Ju YS, et al. Nasal ciliated cells are primary targets for SARS-CoV-2 replication in the early stage of COVID-19. *J Clin Invest.* 2021;131(13):1-14.

16. Alu A, Chen L, Lei H, Wei Y, Tian X, Wei X. Intranasal COVID-19 vaccines: From bench to bed. *eBioMedicine*. 2022; 76:103841.
  17. Kleanthous H, Silverman JM, Makar KW, Yoon IK, Jackson N, Vaughn DW. Scientific rationale for developing potent RBD-based vaccines targeting COVID-19. *npj Vaccines*. 2021;6(1):1–10.
  18. Elias DR, Poloukhine A, Popik V, Tsourkas A. Effect of ligand density, receptor density, and nanoparticle size on cell targeting. *Nanomedicine Nanotechnology, Biol Med*. 2013;9(2):194–201.
  19. Shim S, Yoo HS. The Application of Mucoadhesive Chitosan Nanoparticles in Nasal Drug Delivery. *Mar Drugs*. 2020;18(12):1–17.
  20. Amidi M, Mastrobattista E, Jiskoot W, Hennink WE. Chitosan-based delivery systems for protein therapeutics and antigens. *Adv Drug Deliv Rev*. 2010;62(1):59–82.
  21. Ramasamy R. Innate and Adaptive Immune Responses in the Upper Respiratory Tract and the Infectivity of SARS-CoV-2. *Viruses*. 2022;14(5).
  22. Kaneko N, Kurata M, Yamamoto T, Morikawa S, Masumoto J. The role of interleukin-1 in general pathology. *Inflamm Regen*. 2019;39(1):1–16.
  23. Gubernatorova EO, Gorshkova EA, Polinova AI, Drutskaya MS. IL-6: Relevance for immunopathology of SARS-CoV-2. *Cytokine Growth Factor Rev*. 2020;53(May):13–24.
  24. Jang DI, Lee AH, Shin HY, Song HR, Park JH, Kang TB, et al. The role of tumor necrosis factor alpha (Tnf- $\alpha$ ) in autoimmune disease and current tnf- $\alpha$  inhibitors in therapeutics. *Int J Mol Sci*. 2021;22(5):1–16.
  25. Cesta MC, Zippoli M, Marsiglia C, Gavioli EM, Mantelli F, Allegretti M, et al. The Role of Interleukin-8 in Lung Inflammation and Injury: Implications for the Management of COVID-19 and Hyperinflammatory Acute Respiratory Distress Syndrome. *Front Pharmacol*. 2022;12:1–7.
  26. Student MT, Kumar RR, Ommets REC, Prajapati A, Blockchain T-A, MI AI, et al. Elevated anti-SARS-CoV-2 antibodies and IL-6, IL-8, MIP-1 $\beta$ , early predictors of severe COVID-19. *Front Neurosci*. 2021; 14(1):1–13.
  27. Rossetti M, Gregori S, Roncarolo MG. Granulocyte-colony stimulating factor drives the in vitro differentiation of human dendritic cells that induce anergy in naïve T cells. *Eur J Immunol*. 2010;40(11):3097–106.
  28. Hsu RJ, Yu WC, Peng GR, Ye CH, Hu SY, Chong PCT, et al. The Role of Cytokines and Chemokines in Severe Acute Respiratory Syndrome Coronavirus 2 Infections. *Front Immunol*. 2022;13.
  29. Khader SA, Gaffen SL, Kolls JK. Th17 cells at the crossroads of innate and adaptive immunity against infectious diseases at the mucosa. *Mucosal Immunol*. 2009;2(5):403–11.
  30. Vareille M, Kieninger E, Edwards MR, Regamey N. The airway epithelium: Soldier in the fight against respiratory viruses. *Clin Microbiol Rev*. 2011;24(1):210–29.
  31. Möller I, Michel K, Frech N, Burger M, Pfeifer D, Frommolt P, et al. Dendritic cell maturation with poly(I:C)-based versus PGE2-based cytokine combinations results in differential functional characteristics relevant to clinical application. *J Immunother*. 2008;31(5):506–19.
  32. Castiello L, Sabatino M, Jin P, Clayberger C, Marincola FM, Krensky AM, et al. Monocyte-derived DC maturation strategies and related pathways: A transcriptional view. *Cancer Immunol Immunother*. 2011;60(4):457–66.
  33. Korthals M, Safaian N, Kronenwett R, Maihöfer D, Schott M, Papewalis C, et al. Monocyte derived dendritic cells generated by IFN- $\alpha$  acquire mature dendritic and natural killer cell properties as shown by gene expression analysis. *J Transl Med*. 2007; 5:1–11.
-